DOI: XXX-XXX-XXXX

Mechanism of crack propagation for K9 glass

Xiaoguang Guo[1], Yutong Shi[1,#], Xichun Luo[2,#], Renke Kang[1], Zhuji Jin[1], Fei Ding[2] and Zhipeng Li[3]

1 Key Laboratory for Precision and Non-Traditional Machining Technology of Ministry of Education, Dalian University of Technology, Dalian, China (16024)
2 Centre for Precision Manufacturing, Department of Design, Manufacture and Engineering Management, University of Strathclyde, Glasgow G1 1XJ, UK
3 School of Mechatronics Engineering, Harbin Institute of Technology, Harbin, China
Corresponding Author / E-mail: qq853252184@163.com
Corresponding Author / E-mail: xichun.luo@strath.ac.uk

KEYWORDS : Crack propagation, Critical depth, Initiation crack,Crack delayed growth, SPH simulation

In order to study the mechanism of crack propagation, the varied cutting-depth scratch experiment is carried out and smoothed particle hydrodynamics (SPH) simulation method is used to assistant the investigation. The SPH simulation results reveal that crack will propagate in the direction where stress concentration exceeds the fracture toughness of K9 glass. The initial crack length in critical transition depth is calculated by combining the critical stress of fracture and the fracture toughness of K9 glass. Based on the effective plastic strain, the relation between scratching depth and crack depth is obtained. The recovery of crack tip is found and explained from the relationship between cutting depth and crack depth. Using the energy balance theory of Griffith, the variation of material internal energy is revealed. Comparing the scratching forces obtained from experiment and simulation, the validity of simulation results is verified. The phenomenon of crack delayed propagation is found in both experiment and simulation. The explanation of mechanism is given.

Manuscript received: December XX, 201X / Accepted: August XX, 201X

1. Introduction

K9 optical glass is increasingly used in many sectors such as aerospace, microelectronics and information technology because of its excellent characteristics of high mechanical strength, abrasive resistance, optical transparency, great stability etc. [1]. Ductile regime diamond grinding initiated by Bifano et al [2] is a major processing step for K9 glass in the manufacturing chain and they proposed a theory equation to calculate the brittle-ductile critical transition depth. However, grinding process will still inevitably introduce subsurface damage (SSD) which has to be removed by the following time-consuming polishing process as the SSD will significantly degrade the surface quality and transmission of light. In the past, research was mainly focused on the material removal mechanism and prediction of SSD during grinding of K9 glass. Leng [3] researched the crack morphology of K9 glass by series of grinding experiments and established a model to predict the crack depth based on grinding force and surface quality. Zhang et al [4] investigated the critical depth of cut for K9 glass by varied cutting depth in nano-scratch experiment and calculated the depth of brittle-ductile transition by the value measured from experiment. Besides, they also developed a prediction model for SSD in grinding K9 glass by theoretical derivation and the validity is verified by their grinding experiment [5]. Wang et al [6] researched the influence of ultrasonic assisted machining for K9 glass and proposed a model to predict SSD of K9 glass in rotary ultrasonic face milling. Guo et al [7] established a cutting model of K9 glass by using smoothed particle hydrodynamics method and found the critical cutting depth varied with different tool shape and speed.

Crack propagation is a major step to form the SSD. Understanding mechanism of crack propagation during grinding K9 glass is important to develop measure to mitigate the SSD. However, crack propagation is a dynamic and complex process due to the involvement of interactions of multiple diamond grains and work material in grinding process. It is therefore, very difficult to capture

crack propagation in grinding experiment.

On the other hand, single grain scratching experiment can reveal the fundamentals of the machining process through eliminating the influence of interference from other abrasive grains in the grinding process. To capture the transient dynamic crack propagation, a mesh-free method—smooth particle hydrodynamics (SPH) has been introduced and approved to be an effective method to simulate the single grain scratching process by some researchers. Morten et al [8] proposed the SPH method can be used in metal and gave the parameters of material model. Amir Mir et al [9] using SPH method to research the influence of tool wear on ductile to brittle transition in single point diamond turning and the conclusion has been verified by experiment. Guo et al [10] investigated the distribution law of stress and strain for KDP using different indenters loading by SPH simulation method and the validity was verified by indentation experiments.

In this paper, single diamond grain scratching experiment with the assistant of SPH simulation is carried out in order to gain an in-depth understanding of crack propagation mechanism of K9 glass.

2. SPH Simulation Model and Scratching experiments

2.1 Fundamentals of SPH

Lucy et al. [11] first proposed SPH method in 1977 as one of non-grid numerical simulation methods. Nowadays, it has been widely used in the domains of aviation, optical instrument, automobile manufacturing, petroleum engineering. The key theory of SPH method is interpolation algorithm. Arbitrary macro-variable such as density, temperature, pressure can be represented as the form of integral interpolation by virtue of a group of unordered point. Using core estimated value of scalar field at one point provided by interpolating function it can represent particle movement information. The approximate function of particle at i point can be expressed as

$$\langle f(x_i)\rangle = \sum_{j=1}^{N} \frac{m_i}{\rho_j} f(x_j) W(x_i - x_j, h) \tag{1}$$

Where ρ_j is the density of particle j (j=1,2,…, N), N is the number of particle, j is in the support domain, m_j is the mass of particle j, h is smoothing length and it changes with time and space. W is the core function as illustrated in Fig. 1. It is defined as:

$$W(x,h) = h(x)^{-d}\,\theta(x) \tag{2}$$

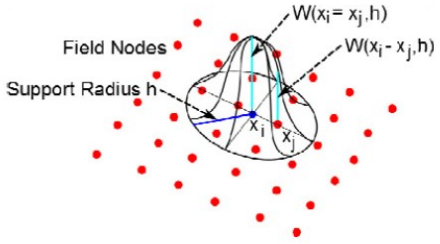

Fig. 1 Kernel function

Where d is space dimensionality. The auxiliary function θ use a cubic spline function which can be expressed as

$$\theta(u) = C \times \begin{cases} 1 - 1.5u^2 + 0.75u^3, & |u| \le 1 \\ 0.25(2-u^3), & 1 < |u| \le 2 \\ 0, & |u| > 2 \end{cases} \tag{3}$$

Where C is a constant.

2.2 Modeling of single-grain scratching process for K9 Glass

The tip radius of indenter used in experiment is 10μm and the indenter contact with K9 glass part is nearly sphere in tip during scratching process. Furthermore, the research focuses on the process of crack propagation. Therefore, the diamond grain is simplified as an ideal spherical rigid body, shown in Fig. 2. The radius of diamond rigid grain is 8μm. Its density is 3.51 g/cm^3 and elastic modulus is 1.141 GPa. The Poisson's ratio is 0.07. For saving computation time and ensuring correctness of simulation, the workpiece of K9 glass is designed as a cube with dimension of 50μm×20μm×30μm. The number of particles in the SPH model is nearly 500,000. The scratching depth is from 0 μm to 5μm and the scratching speed is 1m/s in simulation. The SPH model is constructed by using LS-PrePost.

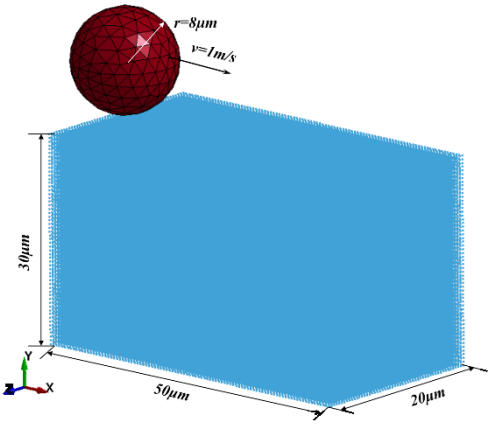

Fig. 2 SPH model of single grain scratching

K9 glass is a kind of hard-brittle material and large-strain damage is in existence in the process of machining. Johnson-Holmquist Ceramics model (JH-2), Johnson-Cook model (JC) and Zerilli-Amstrong model (ZA) are appropriate to large-strain and large-strain rate of material. JC model is expressed as:

$$\sigma = (A + B\varepsilon^n)\left[1 + C\ln\left(\frac{\dot{\varepsilon}}{\dot{\varepsilon}_0}\right)\right]\left[1 - \left(\frac{T - T_0}{T_m - T_0}\right)^m\right] \tag{4}$$

Where A is the yield stress, B is the strength coefficient, C is the strain rate coefficient, n is the strain hardening coefficient, m is the thermal softening coefficient [12].

The constitutive equation of ZA model has two different forms depending on the structure of material such as FCC and BCC. The two kinds of material structures can be described as:

$$\sigma = C_0 + C_1 \exp(-C_3 T + C_4 T \ln\dot{\varepsilon})] + C_5\varepsilon^n \quad \text{(BCC)} \tag{5}$$

$$\sigma = C_0 + C_2\sqrt{\varepsilon}\exp(-C_3 T + C_4 T \ln\dot{\varepsilon}) \quad \text{(FCC)} \tag{6}$$

DOI: XXX-XXX-XXXX

Where C_0 to C_5 and n are six materials constants.

The strain rate, temperature effect such as work hardening, strain-rate hardening and thermal softening are considered in JC model and ZA model [13,14]. This model is appropriate for metal simulation and has been widely used [15,16].

The JH-2 model is used as the constitutive model to study the damage during machining processes and the accumulation of compression failure. The model of non-dimensional strength can be expressed as:

$$\sigma^* = \sigma_i^* - D(\sigma_i^* - \sigma_f^*) \tag{7}$$

Where σ_i^* is the intact material of equivalent stress with non-dimensional, σ_f^* is the destructive equivalent stress of material with non-dimensional, D is damage variable ($0 \le D \le 1$), which can be calculated as

$$D = \sum \frac{\Delta \varepsilon_p}{\varepsilon_p^f} \tag{8}$$

Where $\Delta\varepsilon_p$ is the equivalent plastic strain increment, ε_p^f is the equivalent stress of plastic failure [17]. The marerials constants in the JC model, ZA model and JH-2model have variations because of differenet determination methodologies. The constants in JC and ZA model are considered the influence of temperature [18], but the constants in JH-2 model are defined in room temperature because the temperature have no influence on the brittle materials almostly. The variations will become a source for prediction errors in modeling work.

In the process of single grain scratching, the K9 glass is removed by non-damage plastic deformation firstly, then removed by compression fracture damage. Therefore, JH-2 model is appropriate for used to the simulation of K9 glass. Material properties of K9 glass are shown in Tab.1.

Tab. 1 Material properties of K9 glass [19]

Parameters	Value
Density/(g·cm^{-3})	2.52
Young modulus(GPa)	82
Poisson ratio	0.21
Shear modulus(GPa)	30.4
Tensile strength (GPa)	0.15
Fracture toughness(MPa·m$^{1/2}$)	2.63
Vickers hardness H_v (N/mm^2)	7120
Hug elastic limit(GPa)	5.95

2.3 Scratching experiments

K9 glass samples used in the scratching experiment were prepared by double-surface polishing to obtain good surface quality and flatness on both sides. Its dimension is 25mm×25mm×5mm. The average surface roughness Ra is 1.002nm in the field of 140.66μm×105.49μm measured by a Zygo white light interferometer, as shown in Fig.3.

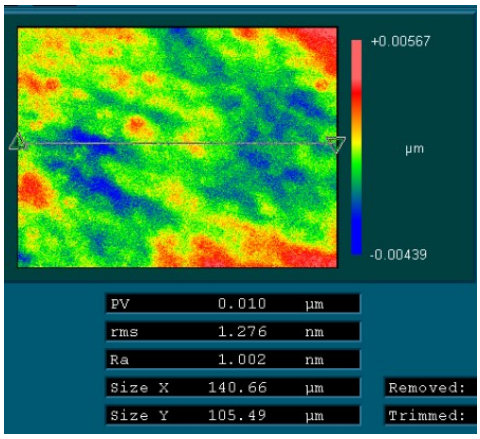

Fig.3 The original surface morphology before scratching

The scratching experiment is taken place on a three-axis ultra precision diamond turning machine, as shown in Fig.4a.The scratching tool is a diamond cone indenter. Its geometrical parameters are shown in Fig.4b. It is fixed on the aerostatic spindle which has been locked into position to present any motion during the scratching process. The K9 workpiece is installed on a Kistler dynamometer which is mounted on an aerostatic bearing slide. The displacement of indenter is recorded by displacement sensor. The scratching speed of indenter is kept at 0.1m/s during the scratching process.

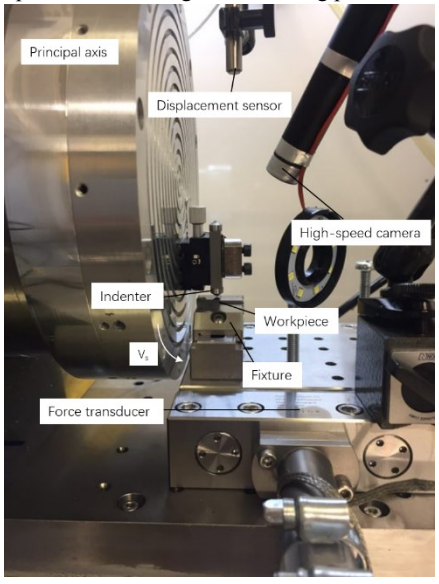

Fig.4a Scratching experiment set-up

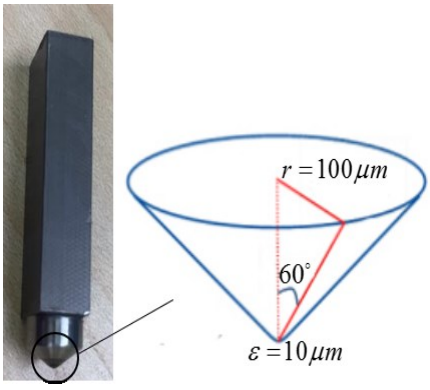

Fig.4b Geometry of indenter

The procedure of scratching experiment is illustrated in Fig.5. In the process of scratching, the work surface will firstly experience elastic deformation and then plastic deformation, although the elastic rebound is still in existence. When the scratching depth goes beyond the critical transition depth, the brittle fracture will occur. In the scratching experiments, the scratching depth will be increased from 0μm to 20μm in a scratching length of 1000μm.

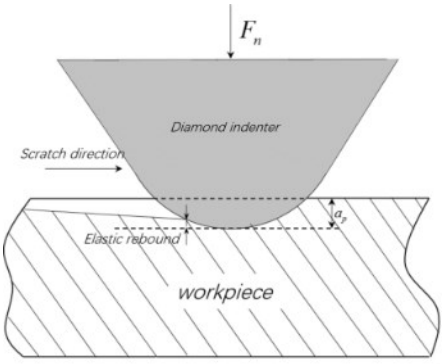

Fig.5 Schematic diagram of scratching procedure

3. Results and discussions

3.1.SPH simulation results

Fig.6 shows the snapshots of SPH simulation and variation of scratching forces under scratching depths of 1.65 μm and 3.9 μm respectively. When the tool contact with K9 glass, brittle fractures can be clearly observed in both cases. Based on the ductile-brittle transition theory proposed by Bifano et al. [2] the critical cutting depth d_c can be calculated by

$$d_c = \beta \frac{E}{H}\left(\frac{K_{IC}}{H}\right)^2 \tag{9}$$

Where E is the elasticity modulus, H is the hardness, K_{IC} is the fracture toughness of the work materials. β is a constant depending on the cutting conditions. β is about 0.15 when cutting hard-brittle materials. According to Eq.6, the critical depth d_c is calculated as *0.2μm*. The critical depth of cut for K9 glass researched by other researchers is about 0.3-1.5μm [5,20]. This is the reason why crack appears.

The initiation crack generated at the scratching depth of 1.65μm observed in plastic strain distribution (as shown in Fig.6(a)). Due to using spherical diamond tool, the scratching process can be regarded as a cutting process under a large negative rake angle cutting tool, which will restrain the occurrence of crack to a large extent. At scratching depth of 3.9μm (as shown in Fig.6(b)), the crack can be clearly observed to propagate along a direction of 45° to the scratching direction. It is because when scratching depth less than critical depth, the scratching force have little difference in normal and tangential direction. The resultant scratching force of tangential force and normal force caused the stress concentration in that direction exceed the fracture toughness of K9 glass. The variation of scratching force and scratching depth is shown in Fig.6(c). It can be seen that the normal force is larger than tangential force but they both increase with the increasing of depth. After a peak value is attained, scratching force has a trend to decrease until it reaches a steady value.

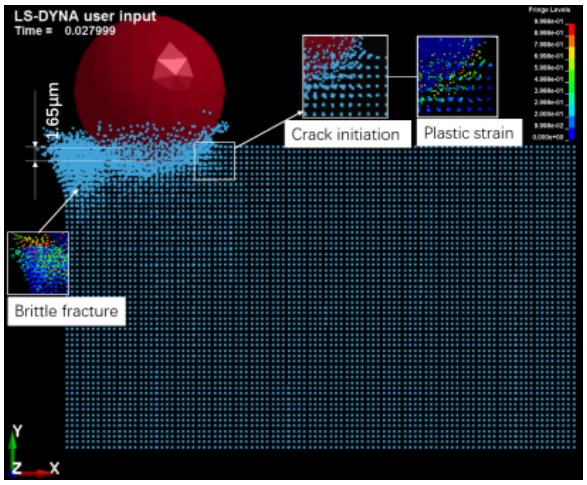

(a). Scratching depth, 1.65μm

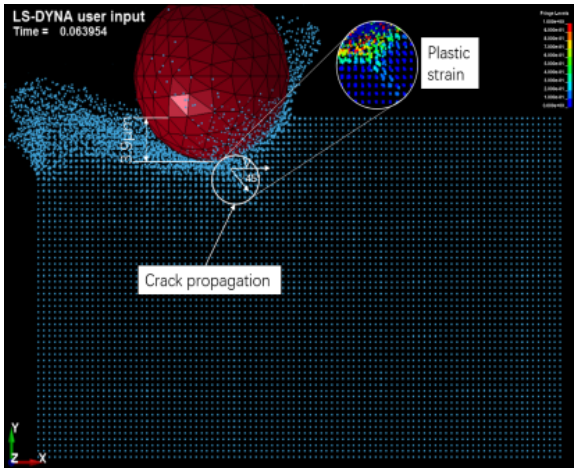

(b). Scratching depth, 3.9μm

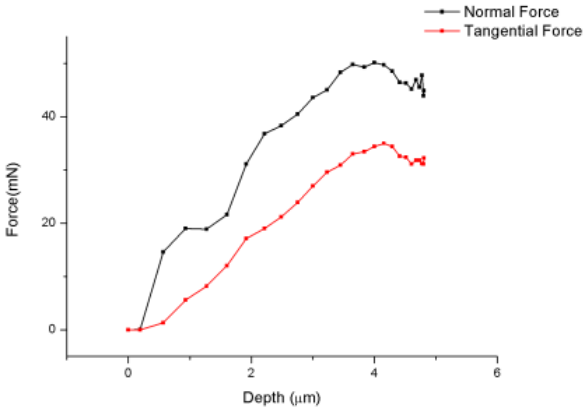

(c). Scratching force with depth

Fig.6 Simulation results

3.2. Crack propagation mechanism

3.2.1. Initial crack length

DOI: XXX-XXX-XXXX

In scratching experiment, it is difficult to capture the transient crack propagation process. Therefore, the SPH simulation is used to analyze the mechanism of crack propagation.

The contact area of diamond grain and workpiece can be seen approximately as a circular area, when the initiation crack is generated (as shown in Fig.7). As the diamond grain is set as a rigid body and has no deformation. The contact area A_c can be expressed as:

$$A_c = \pi\left(\frac{l}{2}\right)^2 \tag{10}$$

Where l in Eq.7 can be calculated as:

$$l = \sqrt{a_p{}^2 + \left(l'/2\right)^2} = \sqrt{a_p{}^2 + r^2 - \left(r - a_p\right)^2} = \sqrt{2ra_p} \tag{11}$$

Where a_p is the cutting depth 1.65μm and r is the radius of diamond grain *8μm*. Therefore, the contact areas A_c can be calculated as $A_c = 20.73\mu m^2$. The normal force F_n in this scratching depth is $36.7993mN$ and the tangential force F_t is $14.9373mN$. The friction coefficient in critical depth can be calculated as :

$$\mu = \tan\alpha = F_t / F_n \tag{12}$$

Where α is the angle between F_n and F_t. The friction coefficient in critical depth is about *0.4*. The resultant force F_r is $39.7154mN$.

The average stress of critical depth in contact area can be expressed as

$$\sigma_a = F_r / A_c \tag{13}$$

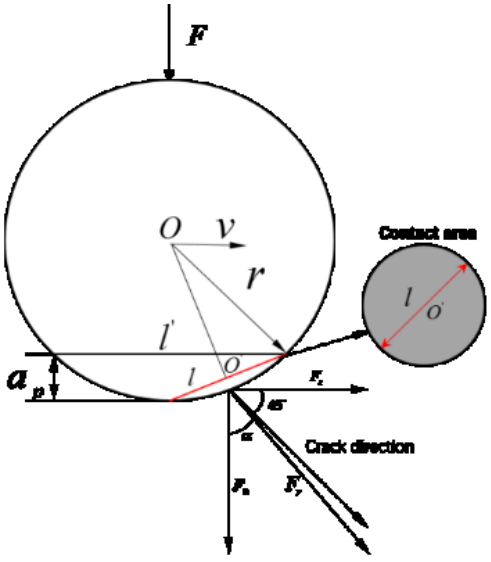

Fig. 7 Schematic diagram of contact area

According to the theory proposed by Lee [21], the maximum Hertzain stress equals to 1.5 times of average stress. It assumes the maximum Hertzain stress appears in critical brittle to ductile transition condition. Therefore, the critical stress of fracture can be obtained as:

$$\sigma_m = 1.5\sigma_a = \sigma_c \tag{14}$$

The K_{IC} of brittle material can be expressed as:

$$K_{IC} = Y\sigma_c\sqrt{\pi a} \tag{15}$$

Where Y is shape coefficient of crack. σ_c is the critical stress in Eq. 13 and $2a$ is the length of initial crack. According to the mechanics of fracture, the crack generated by tensile stress in the vertical crack surface direction is called opening mode crack [22] and Y is *1*. Therefore, from Eq.15, the crack length a can be calculated as

$$a = \left(K_{IC}/\sigma_c\right)^2/\pi \tag{16}$$

In this case, a is 0.26μm and the initiation crack is 0.52μm, which means when the stress reaches the fracture toughness, the crack will grow to 0.5μm directly. This phenomenon indicates that the core crack was in existence interior K9 material and the strength of material is decreased dramatically when the crack is generated.

3.2.2. Effective plastic strain

The plastic strain distribution is obtained during the scratching process, as shown in Fig.8. When the scratching depth is 3.9μm, the crack is generated apparently. The depth of crack is 8.35μm about two times of the scratching depth. With the increase of scratching depth, the depth of crack propagation increased faster than scratching depth. Its growth direction has changed to downward as shown in Fig.8. The stress in normal direction is larger than horizontal direction, which prompts the crack growth downward. When the scratching depth reaches the maximum depth of 4.8μm, the depth of crack is about 11.7μm and the crack propagation direction is almost along the normal direction. After scratching process, the crack depth has grown to 12.2μm and some micro cracks are also generated at the bottom of scratch.

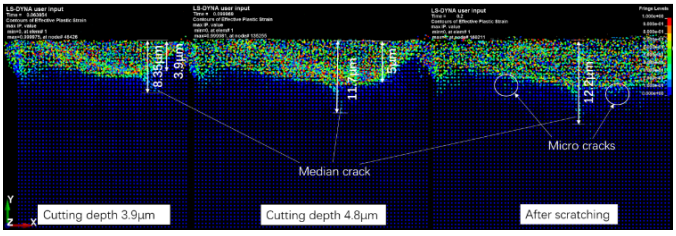

Fig. 8 Effective Plastic Strain

3.2.3. Energy analysis

From macroscopic, the crack is generated and grown by stress concentration at the bottom of the scratch, which exceeds the fracture toughness of material. According to the energy balance theory proposed by Griffith [23], the energy of whole system is consisted of four parts: the work of applied loadings W_L, potential energy of strain U_E, free surface energy U_s, kinetic energy U_k. It can be described as:

$$U = (-W_L + U_E) + U_s + U_k \tag{17}$$

As shown in Fig.9, after the crack starts to generate, the energy of K9 glass workpiece reaches the maximum value. However, this status is unstable. With the propagation of crack, the whole energy is decreased to a steady status. The reason is that the crack propagation will release and transform a part of energy into surface energy of newly formed crack surface. From the microscopic viewpoint, the crack propagation is due to the extra energy exceeding the intermolecular chemical bond energy of material. The bond energy is the intrinsic property of material, but the existence of flow in material will weaken the strength of material greatly.

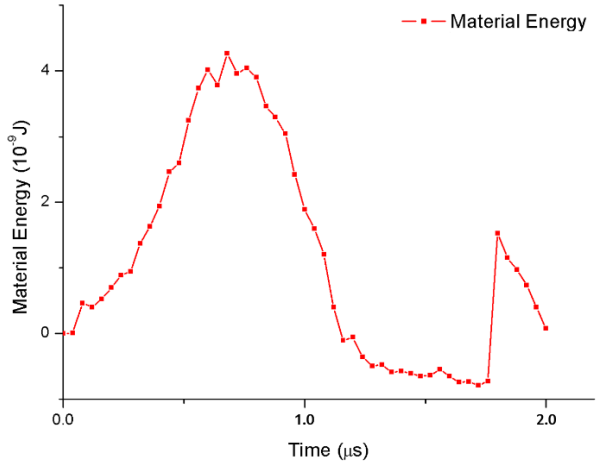

Fig.9 The variation of K9 material energy in scratching proces

3.3. Crack delayed growth

In SPH simulation process, the phenomenon of crack delayed growth was observed. This phenomenon was firstly found by Obreimoff based on mica cleavage experiments [24] where they found that the crack propagation did not reach stable status immediately, but few seconds after, which indicated the importance of chemical kinetics in crack propagation process. In the SPH simulation when scratching depth reached the maximum value, the median crack did not stop growing but continued to grow to a steady status after scratching. This result has been verified by the scratching experiment. The relation of the cutting depth, crack depth and material energy are shown in Fig.10. The initiation crack was generated when the scratching depth of *1.65μm*. Crack grew faster than scratching depth. From point 1 in Fig.10, with the increasing of scratch depth, the material energy reached a peak vaule because the crack did not grow in this depth. When the scratching depth reached the maximum depth of 4.8μm, the crack depth was 11.7μm as shown in point 2 in figure. The crack continued to increase until it reached to a maximum value of 12.8μm with the material energy decreasing rapidly to 0. With the recovery of crack, the maximum depth of crack maintained at 12.2μm and the materila energy reached negative value. This phenomenon is because it takes time for stress to conduct through the material and the variation of internal energy can be verified this explanation.

The model of depths of median crack proposed by Lambropoulos et al. [25] was used to evaluate the SPH simulation. It can be described as:

$$c_m = \alpha_k^{\frac{2}{3}} \left(\frac{E}{H_v}\right)^{\frac{2(1-m)}{3}} (\cot\psi)^{\frac{4}{9}} \left(\frac{F_n}{K_{IC}}\right)^{\frac{2}{3}} \tag{18}$$

Where c_m is the depth of median crack, E is Young modulus, ψ is the tip angle of indenter, H_v is the Vickers hardness, m and α_k are dimensionless factors. The model shows that the depth of median crack is determined by normal force and shape of tool only. In this research, m is set as 1/3 [26], $\alpha_k=0.027+0.09(m-1/3)$. The maximum value of F_n obtained in SPH simulation is 50.1mN. The median crack c_m can therefore, be calculated as 12.6 μm. The Lambropoulos model didn't consider the recovery of crack tip. It results in a slightly larger estimated depth of median crack than the simulated value of 12.2 μm. However, the accuracy of SPH simulation has been approved.

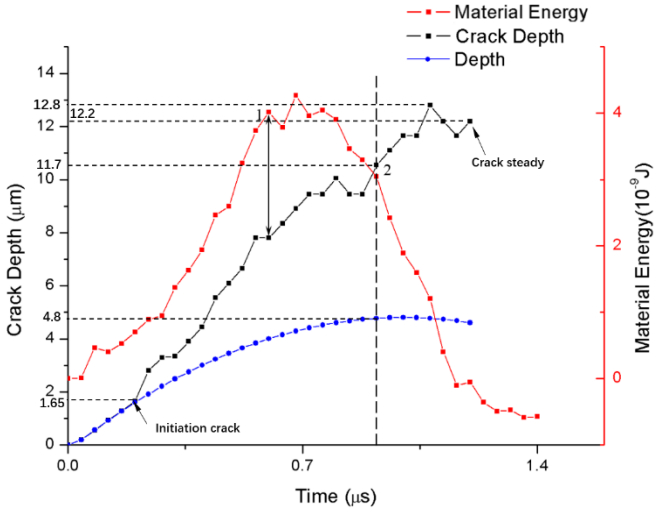

Fig.10 Crack depth, scratching depth and material energy

As illustrated in Fig.11, Lawn et al. [27] believed that lateral crack to analyze the subsurface damage. The median crack was generated in the loading process while the lateral crack was generated in unloading process. This has been approved in the SPH simulation shown in Fig.12.

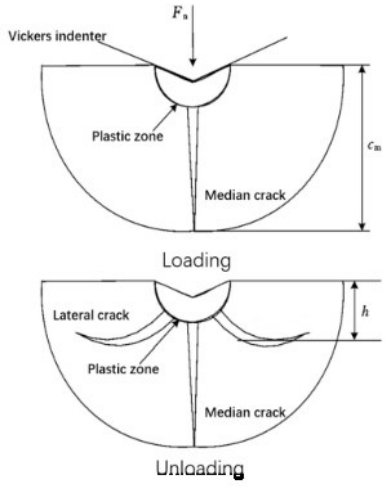

Fig.11 Indentation schematic diagram

DOI: XXX-XXX-XXXX

The lateral crack was observed to generate at section A-A when the diamond tool passed the K9 glass surface in unloading process. At section B-B surface, the diamond tool was scratching the K9 glass surface which can be deemed as the loading process. Median crack growth was observed to appear on this surface section. The Fig.13 showed the distribution of Von Mises stress after scratching. The residual stress influence depth is about 11.15μm, which is shallower than median crack depth. This indicates that the stress can be released at the end of crack but still exist in the region of scratched surface. The growth of crack can lead to the stress relief in the near region. When the diamond tool passed the work surface, high residual stress is generated at the edge of workpiece.

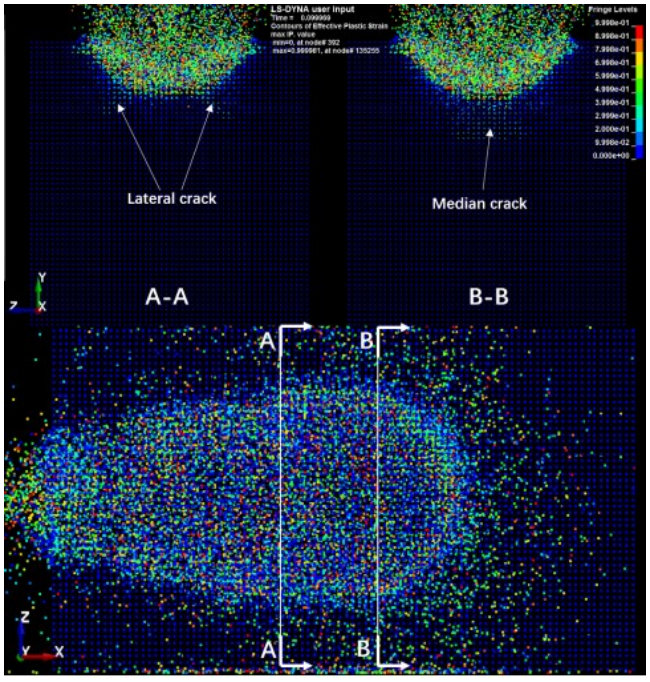

Fig.12 Plastic strain in scratching process

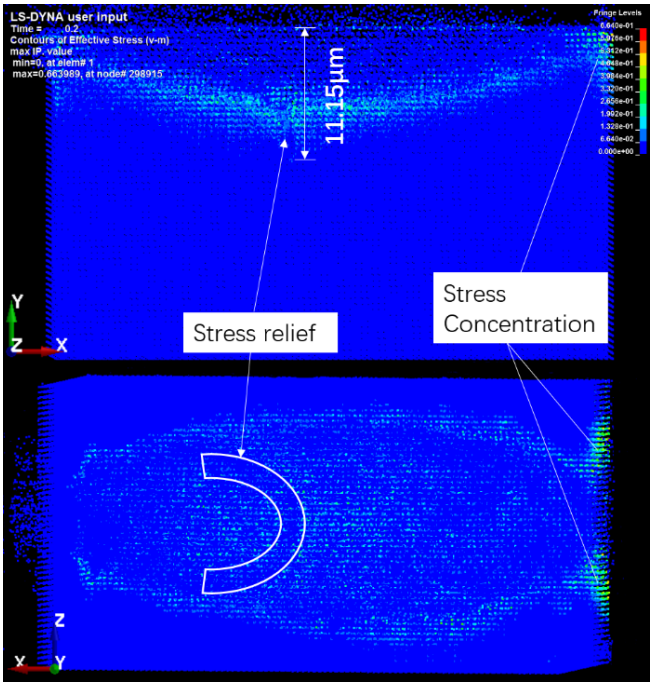

Fig.13 Von Mises stress (Effective stress) in scratching process

4. Validation of SPH model

The validation of SPH model is verified by comparison of the scratching forces. Fig. 14(a) shows the scratching forces obtained by experiment and Fig. 14(b) is simulation forces. In the experiment, the international system of units is used. However, restricted by the model size and scratching depth, the units are μg-μs-μm in simulation. It can be seen that the shape of normal force and tangential force is similar with each other and they all have the same variation tendency. Besides, the ratio of tangential force and normal force is less than 1 in both scratching experiment and simulation results.

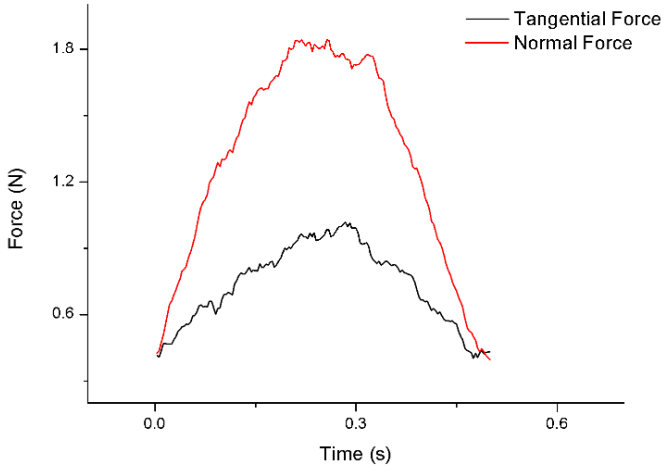

(a) Experiment scratching forces

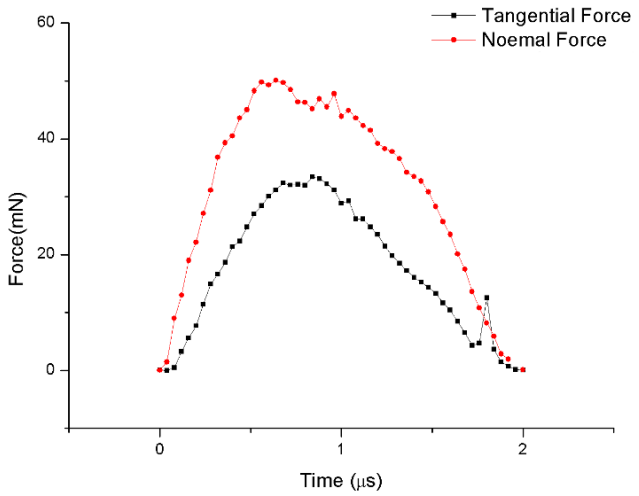

(b) Simulation forces

Fig.14 Comparison of scratching forces obtained by experiment and simulation

The surface topography of scratch is measured by laser scanning confocal microscope, as shown in Fig.15. The plastic deformation is observed at first, then the median crack and lateral crack can be observed, which indicate the brittle fracture occurred. The microcrack is existence on both sides of median crack. The surface topography obtained in scratch experiment is accord with the SPH simulation results, which verify the validity of simulation results.

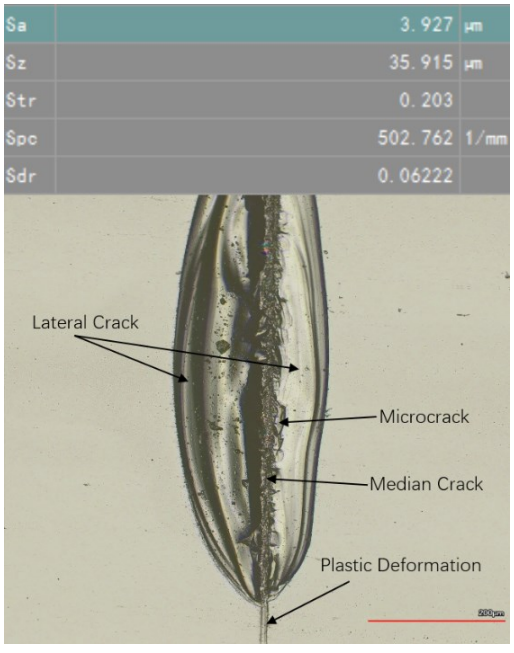

Fig.15 The surface topography after scratch

The validity of simulation results can be further verified by scratching experiment through the so-called crack delayed phenomenon. The phenomenon of crack delayed propagation was observed by high-speed camera in the scratching experiment. In Fig.16(b), after scratching, the median crack can be observed clearly and having no lateral crack can be observed. But the lateral crack grows immediately after scratching. The speed of lateral crack propagation is great fast at first 10 seconds (Fig.16(c-f)), after that, it was slow down and tended to reach static status. About 20s(Fig.16(g)), the morphology of crack had almost no change. The crack propagation process in experiment identified with the simulation process.

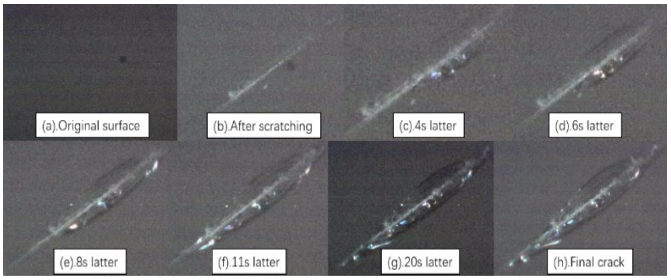

Fig.16 Crack delayed propagation

5. Conclusions

In this paper, the crack propagation process in K9 glass is investigated by both scratching experiment and SPH simulation. The conclusions can be drawn as follows:

(1) The direction of crack propagation is determined by scratching force and scratching depth. Crack will propagate in the direction where stress concentration exceeds the fracture toughness of K9 glass. The initial lateral crack length can be calculated by combining the critical stress of fracture and the fracture toughness of K9 glass, which proposed a method to calculate the length of lateral crack.

(2) The reversibility of crack growth is discovered in K9 glass. This phenomenon can be observed from the relationship between scratching depth and crack depth. The reason about the reversibility of crack growth is given. The variation of material internal energy in scratching process can be revealed based on energy balance theory. Based on the energy, the removal form and crack generation can be predicted. According to the internal energy of material, the point of crack generation can be obtained.

(3) The phenomenon of crack delayed propagation is found in both experiment and simulation. The mechanism is explained that the stress concentration in material is accumulated gradually in scratching process and it takes time to conduct the stress in K9 glass.

(4) Comparing the scratching forces obtained in experiment and simulation, the similar shape and tendency can be observed clearly. The surface topography is consistent with the deformation form of K9 glass in simulation process. The variation of scratching morphology further verifies the existence of crack delayed propagation. The validity of simulation results can be verified.

ACKNOWLEDGEMENT

The authors would like to acknowledge the financial support from the National Natural Science foundation of China (General Program,

DOI: XXX-XXX-XXXX

NO. 51575083 and NO. 51505063), Science Fund for Creative Research Groups (NO. 51621064) and the EPSRC (EP/K018345/1) in the UK.

REFERENCES

1. C. Peirrat, T. Siegrist, J.D. Marco, et al. “Multiple-Layer Blank Structure for Phase-Shifting Mask Fabrication,” J. Vac. Sci. Techn. B, 14:63, 1996.
2. Bifano T. G., Dow T. A., Scattergood R. O. “Ductile-regime grinding: a new technology for machining brittle materials”. Journal of Engineering for Industry-Transactions of the Asme, Vol.113, No.2, pp. 184-189, 1991.
3. Leng B. “Research on grinding subsurface crack and depth prediction of optical glass” [D]. Harbin Institute of Technology,2015.
4. Zhang F. H., Li C., Zhao H. “Prediction Model and Experimental Study of Subsurface Damage Depths in Grinding for K9 Glasses”. China Mechanical Engineering, Vol.27, No.18, pp. 2442-2446, 2016.
5. Zhang F. H., Li C., Meng B. “Investigation of Surface Deformation Characteristic and Removal Mechanism for K9 Glass Based on Varied Cutting-depth Nano-scratch”. Journal of Mechanical Engineering, Vol.52, No.17, pp. 65-71,2016.
6. Wang, J., Zhang, C., Feng, P., & Zhang. “A model for prediction of subsurface damage in rotary ultrasonic face milling of optical k9 glass”. International Journal of Advanced Manufacturing Technology, 83.1-4, pp. 347-355, 2016.
7. Guo Xiaoguang, Wei Yanjun, Jin Zhuji, Guo Dongming. “A numerical model for optical glass cutting based on SPH method”, International Journal of Advanced Manufacturing Technology, 68:1277-1283, 2013.
8. Chong Su, Yu Zhang, Junming Hou, Wanshan Wang. Numerical simulation and analysis for metal cutting processes based on FEM and SPH[P]. System Simulation and Scientific Computing, 2008. ICSC 2008. Asia Simulation Conference - 7th International Conference on,2008.
9. Amir Mir, Xichun Luo, Jining Sun. “The investigation of influence of tool wear on ductile to brittle transition in single point diamond turning of silicon wear”,364-365:233-243, 2016.
10. Guo Xiaoguang, Liu Ziyuan, Gao Hang, et al. “Simulation research of nanoindentation on the (001) face of KDP crystal” [J]. Journal of Synthetic Crystals, 05, pp. 1149-1155, 2015.
11. Lucy L. B. “A numerical approach to the testing of fusion processes” [J]. The Astronomical, 82: 1013-1024, 1977.
12. Jinqiang Ning, Steven Y. Liang. “Model-driven determination of Johnson-Cook material constants using temperature and force measurements” [J]. The international Journal of Advanced Manufacturing Technology. No.97, pp.1053-1060,2018.
13. Tugrul O., Yigit K. “Identification of Constitutive Material Model Parameters for High-Strain Rate Metal Cutting Conditions Using Evolutionary Computational Algorithms” [J]. Materials and Manufacturing Processes.No.22, pp.659-667,2007.
14. Qiang Li, Y. B. Xu, M.N. Bassim. “Dynamic mechanical behavior of pure titanium” [J]. Journal of Materials Processing Technology,155-156, pp.1889-1892,2004.
15. Jingqiang Ning, Vinh Nguyen, et al. “Inverse determination of Johnson-Cook model constants of ultra-fine-grained titanium based on chip formation model and iterative gradient search” [J]. The international Journal of Advanced Manufacturing Technology. No.99, pp.1131-1140,2018.
16. Jinqiang Ning, Steven Y. Liang. “A comparative study of analytical thermal models to predict the orthogonal cutting temperature of AISI 1045 steel” [J]. The international Journal of Advanced Manufacturing Technology.Vol.100, pp.1-11,2019.
17. Johnson G. R, Holmquist T. J. “An improved computational constitutive model for brittle materials” [C]. High-Pressure Science and Technology, Colorado Springs, USA: 981–4, 1994.
18. Jinqiang Ning, Steven Y. Liang. “Prediction of Temperature Distribution in Orthogonal Machining Based on the Mechanics of the Cutting Process Using a Cinstitutive Model” [J]. Journal of Manufracturing and Materials Processing. 2,37,2018.
19. Wang Chengyu. “Handbook of glass materials” [M]. Beijing: Chemical Industrial Press, pp.535-555,2007.
20. P. Yao, Yoshihara N., Hitomi N. “Ductile and brittle mode grinding of fused silica” [J]. Key Engineering Materials. Vol.447-448, pp. 21-25 ,2010.
21. LEE.S.H. “Analysis of ductile mode and brittle transition of AFM nanomachining of silicon”. International Journal of Machine Tools&Manufacyure, pp. 61-71-79, 2012.
22. B. R. Lawn, T. R. Wilshaw. “Fracture of Brittle Solids” [M]. Beijing: Earthquake press: pp. 9-11,1985.
23. Griffith A. A. “Theory of Rupture.” In Proc. First Internat.Congr. Appl. Mech. (ed C.B., Bjezeno&J.M. Burgers), J. Waltman Jr, Delft, pp.55, 1924.
24. Obreimoff, J. W. “The Splitting Strength of Mica.Proces”. Roy. Soc.London, A127,290,1930.
25. Larnbropoulos J. C, Jacobs S. D. “Material removal mechanisms from grinding to polishing”. Ceram Trans. 102:113-128,1999.
26. Wang Z, Wu YuLie, Dai Yifan. “Rapid detection of subsurface damage of optical materials in lapping process and its influence regularity.” Optics and Precision Engineering (01):16-21, 2008.

27. Lawn, B. R. and Evans, A. G., "A model for crack initiation in elastic/plastic indentation fields," Journal of Materials Science, Vol.12, No. 11, pp. 2195-2199,1977.